ELSEVIER

International Journal of Pharmaceutics 167 (1998) 215–221

international journal of pharmaceutics

Effect of particle size and temperature on the dehydration kinetics of trehalose dihydrate

Lynne S. Taylor [1], P. York *

Drug Delivery Group, Postgraduate Studies in Pharmaceutical Technology, School of Pharmacy, University of Bradford, Bradford, West Yorkshire, BD7 1DP, UK

Received 17 November 1997; received in revised form 26 January 1998; accepted 4 February 1998

Abstract

From isothermal thermogravimetric analysis, the dehydration behaviour of different particle size fractions of trehalose dihydrate was investigated between 40 and 90°C. The dehydration rate increased with temperature in accord with the Arrhenius relationship between 40 and 60°C enabling activation energies (E_a) for the dehydration to be calculated for the three particle size fractions studied. The activation energy was found to decrease with particle size with a <45 μm particle size fraction having an E_a approximately 13 kJ/mol lower than a >425 μm sample. It is suggested that the smaller particles contain more lattice defects enabling the water to be released more easily, accounting for the lower E_a. Between 70 and 90°C, the dehydration data showed a non-Arrhenius type behaviour suggesting the mechanism of dehydration changed over this temperature range, in agreement with previous studies.

Keywords: Isothermal dehydration; Trehalose dihydrate; Particle size

1. Introduction

Many pharmaceutical excipients, including sugars, form hydrates which have different physical and chemical properties from their corresponding anhydrates (Khankari and Grant, 1995). Sugars are widely used as excipients during the freeze-drying of liposomes, proteins and small drug molecules. It has been suggested that the ability of some sugars to form hydrates on crystallisation from the amorphous phase, thereby reducing the water content of the remaining amorphous phase, may contribute to an enhanced stabilising potential of that sugar in the dry state (Aldous et al., 1995; Saleki-Gerhardt et al., 1995). It is easy to recognise that an excipient that scavenges water

* Corresponding author. Tel.: +44 1274 384738; fax: +44 1274 384769; e-mail: p.york@bradford.ac.uk

[1] Present address: School of Pharmacy, University of Wisconsin–Madison, 425 N. Charter St., Madison, WI 53706, USA.

0378-5173/98/$19.00
PII S0378-5173(98)00065-9

on crystallisation would enhance the physical and chemical stability of the active substance.

The sugar trehalose has received considerable recent attention as a stabilising agent for labile biological molecules (Crowe et al., 1996). This disaccharide exists as two crystalline forms, a dihydrate and anhydrate and previous studies have shown that, on heating and subsequent dehydration, the dihydrate can either convert directly to the anhydrate or form an amorphous phase which may subsequently crystallise to the anhydrate (Taylor and York, 1998). The route of anhydrate formation was found to depend on the particle size of the sample with large particles converting directly to the anhydrate at a threshold temperature of around 80°C whilst the small particles became amorphous on dehydration. This complex phase behaviour was explained in terms of the effect of particle size on the rate of dehydration and the role that either water or lattice disorder (resulting from dehydration) may play in the crystallisation to the anhydrate at the conversion temperature. However no quantitative studies on the kinetics of dehydration were reported.

The influence of particle size on the solid state phase behaviour of trehalose dihydrate on dehydration suggests that the mechanism of dehydration may likewise be influenced by particle size. Varying the particle size has previously been observed to affect the dehydration mechanism in the case of theophylline monohydrate (Agbada and York, 1994) and kinetic studies enable predictions to be made with regard to the rate and probable mechanism of dehydration. Thermal dehydration is usually treated as a solid state decomposition reaction of the type shown in Eq. (1) with the hydrate regarded as a solid which on heating produces water vapour and solid anhydrous material.

$$A.H_2O(s) \rightarrow A(s) + H_2O(v) \quad (1)$$

Solid-state decomposition reactions can be classified by one of four mechanisms; (i) nucleation controlled, (ii) diffusion controlled, (iii) phase boundary and (iv) order reactions (Byrn, 1982). If the fractional dehydration can be determined experimentally at different temperatures, the data can be analysed using the kinetic models of reaction mechanisms known to occur in the solid state (Sharp et al., 1966).

The aim of this study was to obtain kinetic data on the dehydration of trehalose dihydrate over a range of temperatures and to investigate the influence of particle size on both the activation energy of dehydration, E_a and the mechanism of dehydration.

2. Materials and methods

2.1. Materials

αα-Trehalose (α-D-glucopyranosyl α-D-glucopyranoside) was obtained as the dihydrate from Pfanstiehl (Waukegan, IL, USA). This material was used as supplied in this study, but it is known that the powder underwent a milling operation during production.

2.2. Methods

2.2.1. Particle size fractionation

A nest of sieves (Endecott, London, UK) was used to separate trehalose dihydrate into a series of particle size fractions. Sieves of apertures 425, 250, 150, 75 and 45 μm were stacked and 200 g of powder was sieved for 30 min using an Endecott mechanical sieve shaker. Particle size fractions that were >425 and <45 μm, in addition to the unfractionated material were utilised in this study.

2.2.2. Isothermal thermogravimetric analysis

Isothermal dehydration of samples was monitored using a Perkin Elmer TGA 7 Thermogravimetic Analyser (Perkin Elmer, Beaconsfield, UK). The temperature was calibrated using the ferromagnetic standard supplied by Perkin Elmer. Samples (7.5 ± 0.5 mg) were analysed in a flame-cleansed open platinum pan under a dry nitrogen purge. Isothermal scans were obtained in triplicate at 40, 45, 50, 55, 60, 70, 80 and 90°C. For each experiment, the TGA furnace was heated rapidly at 150°C/min to

Table 1
Kinetic equations of the most common mechanisms of solid state decompositions (compiled from Sharp et al., 1966)

Symbol	Equation	Rate-controlling process
P1	$\ln x/(1-x) = kt$	Random Nucleation, Prout–Tompkins
A2	$[-\ln(1-x)]^{1/2} = kt$	Two-dimensional nucleation, Avrami–Erofeev, $n = 1/2$
A23	$[-\ln(1-x)]^{2/3} = kt$	Two-dimensional nucleation, Avrami–Erofeev, $n = 2/3$
A3	$[-\ln(1-x)]^{1/3} = kt$	Two-dimensional nucleation, Avrami–Erofeev, $n = 1/3$
A4	$[-\ln(1-x)]^{1/4} = kt$	Two-dimensional nucleation, Avrami–Erofeev, $n = 1/4$
F1	$-\ln(1-x) = kt$	Random nucleation, first order mechanism
R1	$1-x = kt$	Phase boundary reaction, zero order mechanism
R2	$1-(1-x)^{1/2} = kt$	Phase boundary reaction, cylindrical symmetry
R3	$1-(1-x)^{1/3} = kt$	Phase boundary reaction, spherical symmetry
D1	$x^2 = kt$	One dimensional diffusion
D2	$(1-x)\ln(1-x)+x = kt$	Two dimensional diffusion
D3	$[1-(1-x)^{1/3}]^2 = kt$	Three dimensional diffusion, Jander equation
D4	$1-(2/3)x-(1-x)^{2/3} = kt$	Three dimensional diffusion, Ginstling–Brounshtein equation

reach the required temperature and the sample was maintained at this temperature until dehydration was complete. After heating to the experimental temperature, a short period was required to stabilise the balance prior to data collection during which some dehydration occurred, accounting for slightly lower than expected values of weight loss, especially at higher temperatures.

2.2.3. Analysis of dehydration data

Results were analysed based on the method of Agbada and York (1994). The fractional dehydration (x) in the range 5–80% was measured at known times (t) for the different experimental temperatures. These data were plotted according to the kinetic equations shown in Table 1 and the conformity of the plots assessed by least-squares correlation coefficients (r). Data over the fractional dehydration range 5–50% were also analysed. The equations giving the best fits were then used to obtain kinetic parameters. The slopes of the linear plots at the various isothermal dehydration temperatures correspond to the dehydration rate constants. The activation energy of the dehydration was estimated from an Arrhenius plot of the rate constants obtained between 40 and 60°C, determined using data over the range 5–80% fractional dehydration, although essentially no change in the slope of the Arrhenius plot was observed when 5–50% data were used in the analysis.

3. Results

3.1. Influence of temperature on dehydration profile

Fig. 1 shows representative fractional dehydration plots for the <45 μm particle size fraction between 40 and 60°C. As expected, the rate of dehydration increases as the experimental temper-

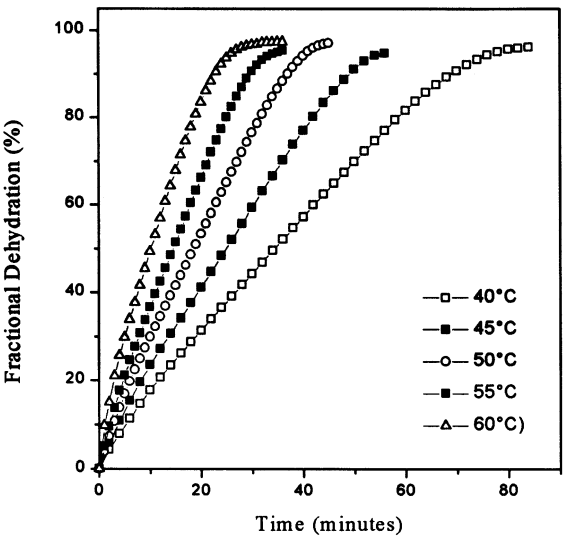

Fig. 1. Representative isothermal dehydration curves of trehalose dihydrate <45 μm powder over the temperature range 40–60°C.

ature is raised. The other two particle size fractions produced qualitatively similar plots (data not shown). When compared at equivalent temperatures, the rate of dehydration increases in the order (<45 μm) > unfractionated > (>425 μm).

Fig. 2 displays typical curves obtained between 60 and 90°C for the three different particle sizes. The dehydration behaviour is more complex across this temperature range with the dehydration rate showing a different dependence on temperature than for between 40 and 60°. For the >425 μm and unfractionated samples, the rate of dehydration at 70°C is approximately the same as at 60°C, whilst at 80°C the dehydration rate is noticeably slower than at 60°C. This slower rate of dehydration is especially pronounced in the >425 μm sample (see Fig. 3). At 90°C the dehydration occurs most rapidly and it would appear that significant dehydration occurs during the equilibration period prior to data collection since the extent of dehydration does not reach 100%. In the case of the <45 μm particle size fraction, the dehydration rate reaches a minimum at 70°C and then increases at 80 and 90°C.

3.2. Analysis of dehydration data

Dehydration data, over the range 5–80% fractional dehydration, were analysed in terms of the equations shown in Table 1. It was found that, in contrast to data obtained for studies between 40 and 60°C, good fits to any of the equations shown in Table 1 could not be obtained with data obtained at temperatures greater than 70°C. Good fits to the data over the entire temperature range could however be obtained by fitting only the initial dehydration data. Fig. 3 shows an Arrhenius plot for the >425 μm and <45 μm particle size fractions. Clearly the temperature dependence of the rate constants for dehydration changes between 60 and 70°C for both particle size fractions, with a break in linearity, although the effect is more dramatic for the larger particle size fraction. Thus Arrhenius plots were therefore con-

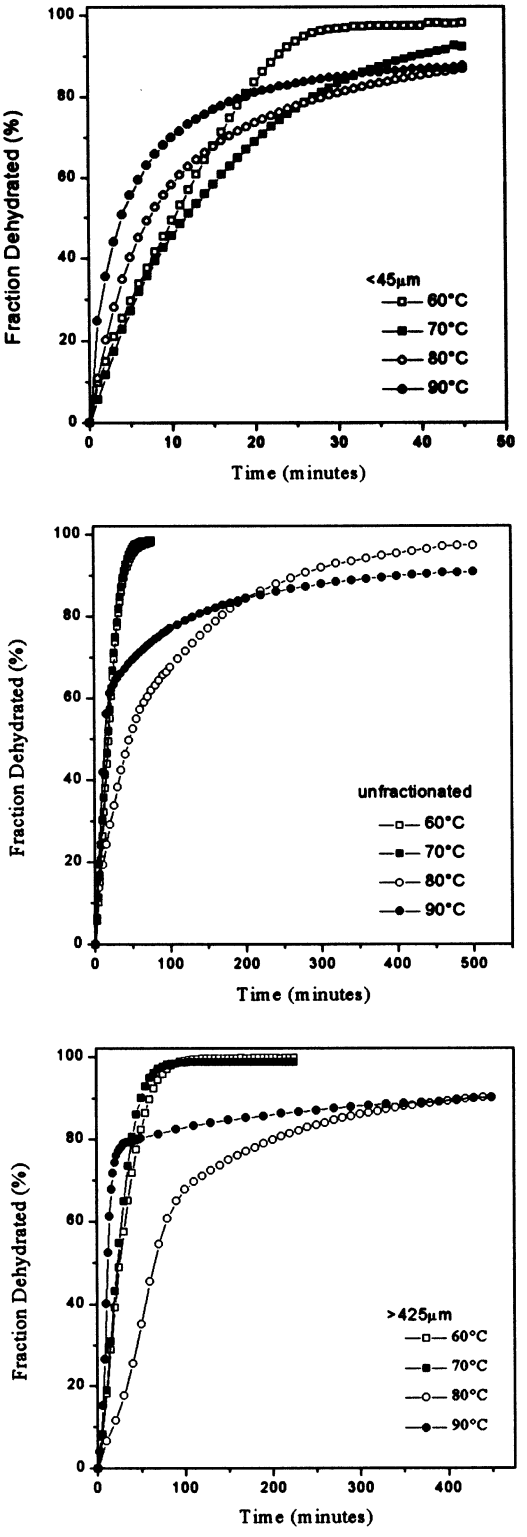

Fig. 2. Representative isothermal dehydration curves of >425 μm, unfractionated and <45 μm trehalose dihydrate powder over the temperature range 60–90°C.

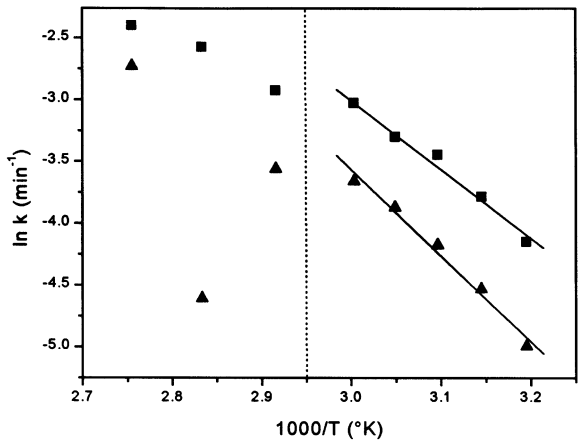

Fig. 3. Arrhenius plot of rate constants calculated using the A2 equation and fractional dehydration data between 5 and 50% for >425 μm (▲) and <45 μm (■) trehalose dihydrate. Rate constants were determined at temperatures between 40 and 90°C and the dotted line shows where the dehydration mechanism alters resulting in an Arrhenius plot that is no longer linear at temperatures above 60°C.

structed only from data obtained between 40 and 60°C, using rate constants determined from the equations which gave the best fits. The Arrhenius plots for <45 μm trehalose dihydrate are shown in Fig. 4. Good fits to the dehydration data for the <45 μm and unfractionated samples were obtained with the Avrami equation and the phase

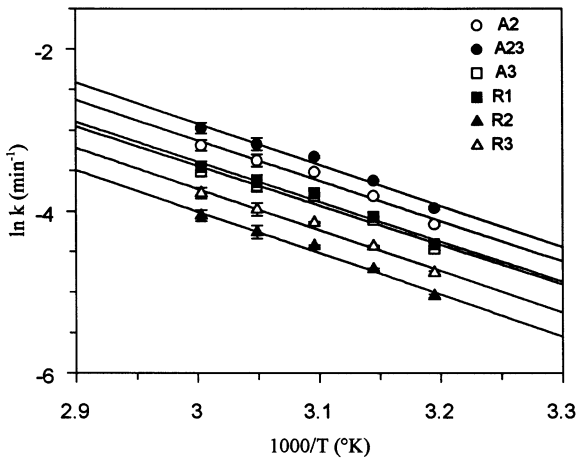

Fig. 4. Arrhenius plot of best fitting dehydration mechanisms for <45 μm trehalose dihydrate. The data are mean values where $n=3$ and the error bars represent the standard deviation of the data. (See Table 1 for definition of symbols).

boundary models. For the >425 μm sample, in addition to these models the one dimensional diffusion equation also gave a good fit. The activation energy (E_a) of dehydration for the three particle size fractions, calculated using the best fitting equations, are shown in Table 2. The activation energy for dehydration varies with particle size with the <45 μm particle size fraction having a E_a approximately 13 kJ/mol lower than that of the >425 μm sample. Within experimental error, there is no difference in the values of the activation energies calculated using the different dehydration models.

4. Discussion

Several dehydration models provide good fits to the experimental data between 40 and 60°C and thus little information about the mechanism of dehydration can be gained from this analysis. These different models do however yield similar activation energies, even between the various model types. Ledwidge and Corrigan (1996) have recently commented on a lack of discrimination of the different best fitting models.

The trend observed in the decrease in the activation energy with a decrease in particle size has been noted with theophylline monohydrate and it was suggested that this could be due to the enhanced dehydration from the greater surface to mass/volume ratio of the smaller particles (Agbada and York, 1994). However the magnitude of the observed decrease in E_a with decreasing particle size is much larger for trehalose dihydrate than for theophylline monohydrate, where a change of only 2.5 kJ/mol was observed when the particle size was decreased from <500 to <150 μm. The degree of disorder in crystals has also been shown to have a significant effect on the dehydration behaviour of organic hydrates with lattice defects facilitating water removal (Hüttenrauch and Fricke, 1981). For example, grinding cefixime trihydrate for 4 h was found to decrease the E_a by approximately 20 kJ/mol (Kitamura et al., 1989). It is likely that the decrease in the E_a for the smaller particle size fraction of trehalose dihydrate reflects a greater disorder in the crystal

Table 2
Activation energy (E_a) for the dehydration of different particle size fractions of trehalose dihydrate

Dehydration mechanism	<45 μm E_a (kJ/mol)	Unfractionated E_a (kJ/mol)	>425 μm E_a (kJ/mol)
Avrami–Erofeev ($n=2$)	41.1 (2.5) $r=0.988$	50.1 (1.3) $r=0.980$	56.1 (2.7) $r=0.997$
Avrami–Erofeev ($n=2/3$)	42.2 (2.6) $r=0.991$	51.1 (2.1) $r=0.981$	55.1 (2.5) $r=0.994$
Avrami–Erofeev ($n=3$)	40.7 (4.8) $r=0.982$	—	55.1 (2.2) $r=0.994$
One dimensional phase boundary	41.1 (2.3) $r=0.988$	51.1 (2.4) $r=0.98$	—
Two-dimensional phase boundary	42.1 (2.5) $r=0.992$	51.1 (2.1) $r=0.981$	55.1 (2.1) $r=0.993$
Three-dimensional phase boundary	42.1 (2.6) $r=0.994$	51.1 (2.2) $r=0.982$	55.1 (1.8) $r=0.998$
One-dimensional diffusion	—	—	55.1 (2.6) $r=0.993$

The values in parentheses represent the standard deviation of the data where $n=3$.

lattice of these particles. The material is known to have been milled during production and the smaller particles, resulting from more extensive milling than the larger particles, will be more disordered and undergo more facile dehydration. Analysis of activation energies for dehydration may provide information about the extent of disorder in processed samples. An awareness of sample history is obviously also of paramount importance when interpreting parameters such as activation energy and the values reported in this study will reflect the processing history of the material.

The change in the dependence of the dehydration rate with temperature at 70°C indicates that the dehydration mechanism alters in this temperature region. Previous studies have found that it is possible to directly transform trehalose dihydrate into the anhydrate at around 80°C (Taylor and York, 1998). At lower temperatures, the material dehydrated without recrystallisation to the anhydrate, producing a disordered product phase. The change in the dehydration kinetics above 70°C is unsurprising given the observed change in the product phase formed on dehydration around this temperature region.

The decrease in the rate of dehydration over the 70–80°C temperature range, which is especially pronounced with the large particles at 80°C is of particular interest. The new solid state product phase, i.e. the anhydrate, presumably formed at the surface, may be less permeable to water diffusion, thus impeding dehydration. Alternatively, the liberated water molecules might be involved in the rearrangement of the dihydrate to the anhydrate as discussed previously (Taylor and York, 1998), resulting in a slower dehydration rate. The non-linearity of the dehydration rate of the <45 μm particle size fraction with temperature, although not as pronounced in the large particle size fraction, is somewhat surprising, based on previous observations that this material becomes disordered on dehydration and does not convert to the anhydrate at 80°C (Taylor and York, 1998). There may be a small quantity of material converted to the anhydrate, not detected previously, which results in the observed non-Arrhenius behaviour. Another explanation may be related to the fact that when the sample is rapidly heated to the temperature of analysis in this study, it has less time to dehydrate on reaching the threshold temperature for conversion, with most of the dihydrate water retained. In contrast, in prior work (Taylor and York, 1998) the powder dehydrated to a greater extent during slower heating at 10°C/min. It has been suggested that the presence of the dihydrate water is necessary to enable rearrangement to the anhydrate, perhaps through maintaining the structural integrity of the lattice (which is lost during dehydration at lower temperatures), or possibly through a more direct involvement in the rearrangement to the anhydrate (Taylor and York, 1998). The extent of dehydration at the conversion temperature is therefore considered to play a role in determining the ability of the material to transform to the anhydrate, and this is affected by the experimental conditions.

5. Conclusions

The kinetics of dehydration of three particle size fractions of trehalose dihydrate were monitored between 40 and 90°C. The relationship between temperature and the rate of dehydration alters at around 70°C for all the powders studied, indicating that the dehydration mechanism changes in this temperature region. These results are consistent with previous studies examining the phase behaviour of trehalose dihydrate following dehydration (Taylor and York, 1998) and can be explained by a change in the product phase from a disordered to crystalline anhydrous material. The activation energy for the dehydration of trehalose dihydrate, calculated from dehydration data generated between 40 and 60°C, decreases considerably with a decrease in particle size. This is attributed mainly to an increased number of lattice defects in the smaller particles, caused by mechanical processing, that facilitate the water removal.

Acknowledgements

The authors gratefully acknowledge EPSRC and SmithKline Beecham for the provision of a CASE award for LST. Mrs J. Pedley is thanked for assistance with TGA measurements.

References

Agbada, C.O., York, P., 1994. Dehydration of theophylline monohydrate powder—effects of particle size and sample weight. Int. J. Pharm. 106, 33–40.

Aldous, B.J., Auffret, A.D., Franks, F., 1995. The crystallisation of hydrates from amorphous carbohydrates. Cryo-Lett. 16, 181–186.

Byrn, S.R., 1982. Solid State Chemistry of Drugs. New York, Academic Press.

Crowe, L.M., Reid, D.S., Crowe, J.H., 1996. Is trehalose special for preserving dry biomaterials? Biophys. J. 71, 2087–2093.

Hüttenrauch, R., Fricke, S., 1981. The influence of lattice defects on the course and rate of drying of particulate solids. Int. J. Pharm. Tech. Prod. Mfr. 2, 35–37.

Khankari, R.K., Grant, D.J.W., 1995. Pharmaceutical hydrates. Thermochim. Acta 248, 61–79.

Kitamura, S., Miyamae, A., Koda, S., Morimota, Y., 1989. Effect of grinding on the solid-state stability of cefixime trihydrate. Int. J. Pharm. 56, 125–134.

Ledwidge, M.T., Corrigan, O.W., 1996. Effects of environmental factors on the dehydration of diclofenac HEP dihydrate and theophylline monohydrate. Int. J. Pharm. 147, 41–49.

Saleki-Gerhardt, A., Stowell, J.G., Byrn, S.R., Zografi, G., 1995. Hydration and dehydration of crystalline and amorphous forms of raffinose. J. Pharm. Sci. 84, 318–323.

Sharp, J.H., Bridley, G.W., Narahari Achar, B.N., 1966. Numerical data for some commonly used solid state reaction equations. J. Am. Ceram. Soc. 49, 379–382.

Taylor, L.S., York, P., 1998. Characterisation of the phase transitions of trehalose dihydrate on heating and subsequent dehydration. J. Pharm. Sci. 87, 347–355.